Supplementary Data Figures

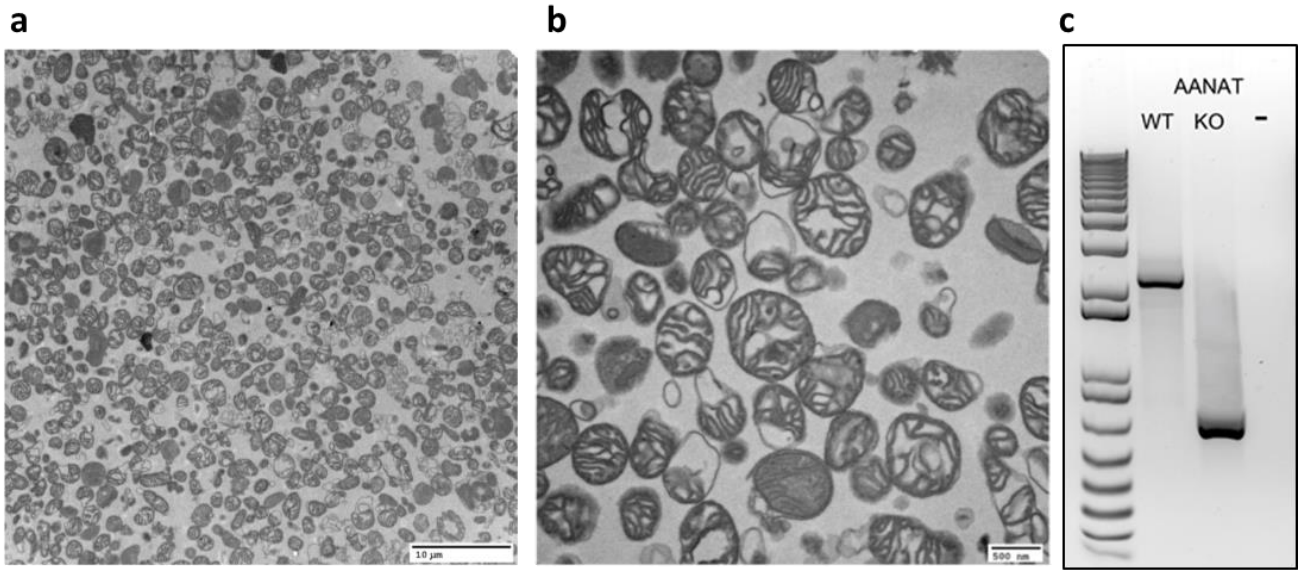

Supplementary Data Figure 1. Purity of mitochondrial preparation from mouse brain and Knockout confirmation. a, b, Percoll gradient purified brain mitochondria imaged using electron microscopy. Samples were examined for mitochondrial morphology, which is normal, and for the presence of contaminating membranes, which were not found. This data supports the immunoblot data in Fig. 1 showing that nonsynaptosomal fractions are pure. Scale bar is 10 μm (**a**) or 500 nm (**b**). **c,** Generation of AANAT-KO N2A cells. N2A cells were incubated with gRNAs designed to knock out AANAT. After incubation, cells positive for transient transfection based on fluorescence were singly-sorted into a 96 well plate using a FACS sorter. Clonal colonies were expanded and an aliquot were subjected to RT-PCR for AANAT. The absence of the full length band and the appearance of the truncated band demonstrate AANAT-KO. WT cells were run as a positive control for AANAT and a no-DNA negative control was also run.

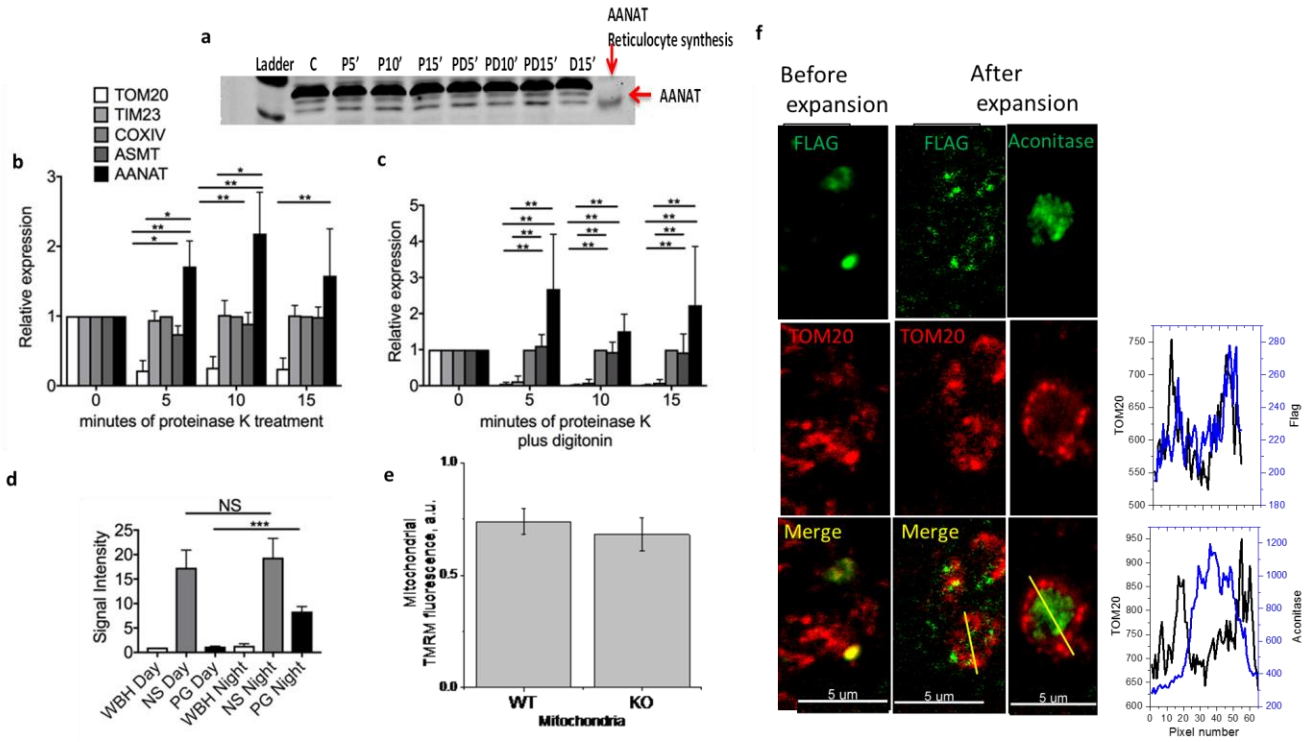

Supplementary Data Figure 2: Quantification of key enzymes in melatonin synthesis after immunoblotting of lysates following proteinase K or proteinase K plus digitonin digestion.

a, AANAT immunoblot with positive control. Non-synaptosomal mitochondria from six week-old B6CBA mice were incubated with proteinase K (P) or proteinase K+digitonin (PD) for the times indicated. Untreated control (C) and digitonin only (D) are also shown. Lane 10 is a positive control of in vitro synthesized AANAT. Following digestion, protease inhibitors were added and lysates subjected to immunoblotting, n=3. In vitro synthesis was done using a rabbit reticulocyte transcription and translation kit with a eukaryotic expression vector for AANAT. **b,** Non-synaptosomal mitochondria from six week-old B6CBA mice were incubated with proteinase K for the times indicated, n=3. **c,** Non-synaptosomal mitochondria from six week-old CBA mice were incubated with proteinase K and digitonin for the times indicated, n=3. Following digestion, protease inhibitors were added and lysates subjected to immunoblotting, n=3 (representative blot in figure 1B). Quantification was performed using fluorescence values

from LiCor detection. To control for loading, all values were normalized by COXIV values, then expressed as relative to untreated control (0 min of proteinase K treatment). Statistical analysis was done using ANOVA to correct for multiple comparisons, followed by posttest analysis. *indicates confidence interval of >95%, **indicates confidence interval of >99%. **d,** Quantification of day and night AANAT proteins from WBH, non-synaptosomal mitochondria and pineal gland using fluorescence values of immunoblots detected by LiCor machine. All values are normalized to beta-actin or COXIV, n=3 (representative blot in figure 1c). ***$p<0.001$. **e,** Assessment of the mitochondrial membrane potential of mitochondria isolated from wild type (WT) and AANAT knock-out (KO) N2a cells. Isolated mitochondria (0.125 mg/mL) were incubated for 15 min with 1 μM TMRM in the buffer containing 5mM Glutamate/Malate as respiratory substrate. Then mitochondria were spun down and TMRM fluorescence ($\lambda_{ex/em}$=550/590) was assessed in the supernatant. The supernatant TMRM fluorescence measured after incubation of mitochondria with 0.5 μM FCCP was taken as maximum $\Delta\varphi_m$ -dependent mitochondrial capacity for TMRM accumulation. The panel shows an average of n=4 biological repeats and standard deviation is shown as error bars. **f,** Expansion microscopy and plot demonstrating that staining intensity of MT1 correlates with TOM20, but not aconitase, consistent with co-localization. Expansion microscopy of mitochondria isolated from MT1-FLAG transfected N2a cells then fixed with 4% PFA for 5 min and permeabilized with Triton X-100 for 10 min. Left column shows mitochondria before expansion, and middle column demonstrate mitochondrial immunostaining of MT1-FLAG and TOM20 after expansion. Control panels (right column) demonstrate aconitase staining in the mitochondrial matrix and TOM20 staining on the outer membrane. Line scan graphs show the immunofluorescence intensities along mitochondrion.

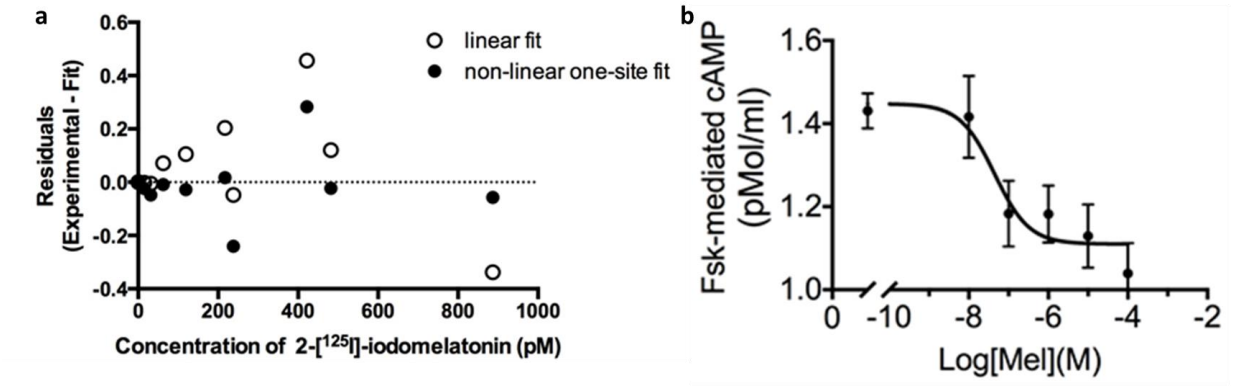

Supplementary Data Figure 3: Characterization of MT_1 receptor binding and function. a, Residual plots comparing linear and non-linear 1-site fit. Residual sum of squares was lowest for non-linear regressed curves 1-site fit (SS=0.145982) vs. linear regressed lines (SS=0.396595). F-tests demonstrate that the data fit significantly better to nonlinear regressed graphs v.s linear. Ratio (F) = 12.02 (p= 0.01). **b,** Signaling properties of mitochondria MT1. Concentration-response effect of melatonin on forskolin (Fsk, 10 µM)-mediated cAMP on isolated mitochondria. Data represent the mean values value ± s.e.m of N = 6 experiments.

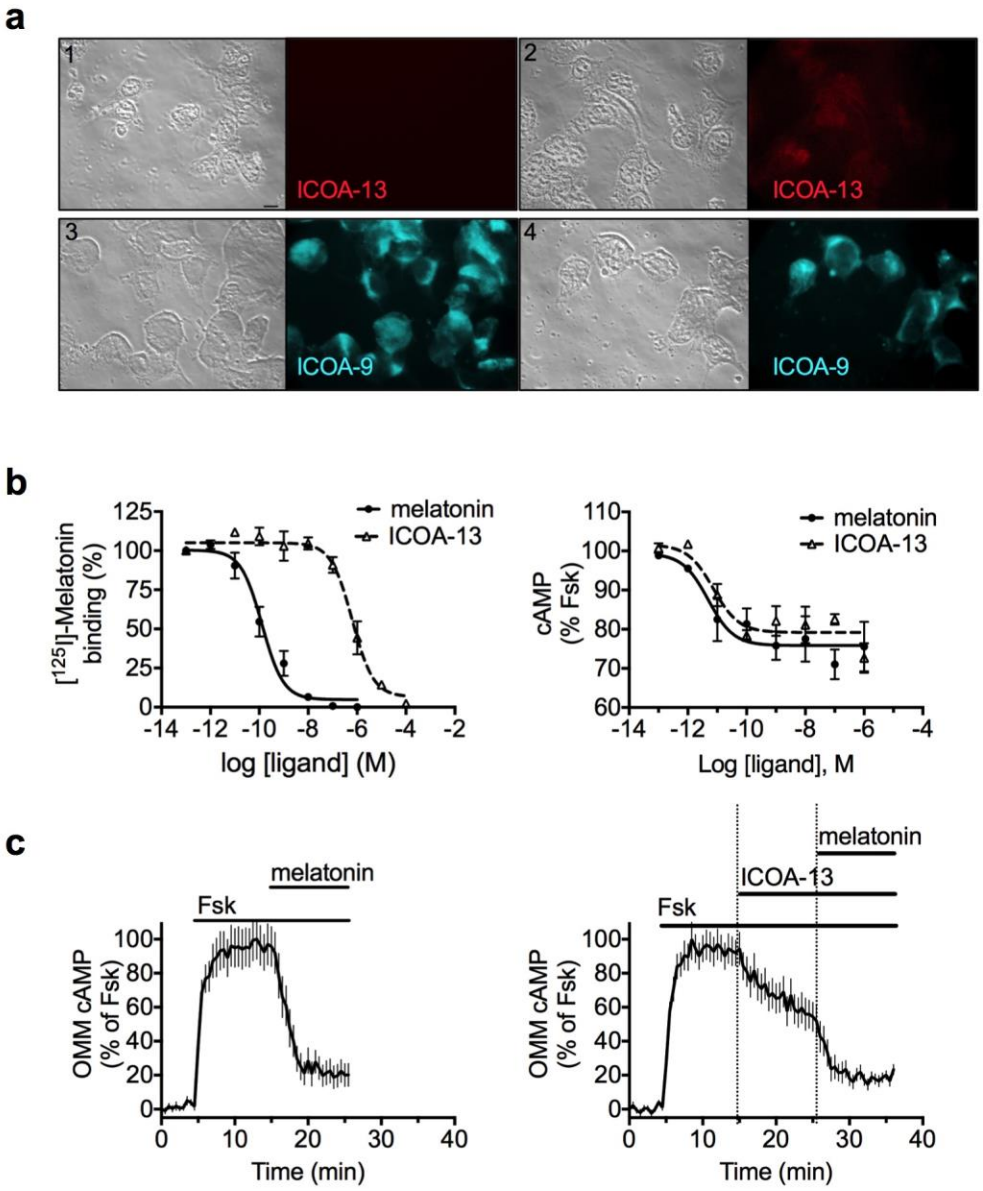

Supplementary Data Figure 4: Characterization of ICOA-13. a, Bright-field and corresponding fluorescent images of HeLa cells incubated with 100 nM of the cell non-permeant melatonin analog, ICOA-13 (1,2), or its cell permeant analog, ICOA-9 (3,4), for 4h under non-permeabilized conditions (1,3) or permeabilized conditions (2,4) (Triton 0.2%). **b**, Competition binding isotherm assays in membrane preparation from HEK293T cells expressing mouse MT_1, and concentration-response curves of melatonin (MT) and ICOA-13 (30 min) on Fsk-stimulated cAMP production measured by HTRF assay in the same cells. Data expressed as the mean value

± s.e.m., from 3-4 independent experiments. **c**, Averaged time courses of Fsk-mediated cAMP production in N2a cells expressing MT_1 and the OMM localized FRET-based cAMP biosensor and challenged by melatonin (MT) and ICOA-13. Data expressed as the mean value ± s.e.m., from n=50 cells.

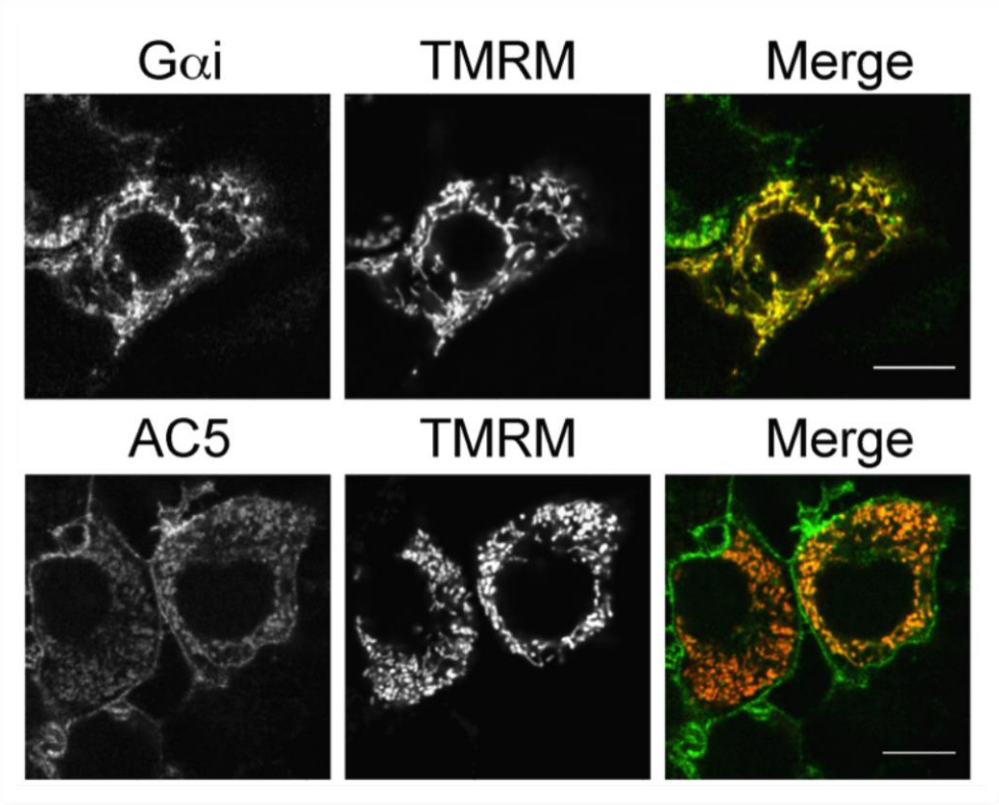

Supplementary Data Figure 5. Localization of GαI and AC5 in neuroblastoma cells.

Confocal imaging of neuroblastoma N2a cells expressing Gαi-GFP or AC5-YFP (green) together with the matrix mitochondrial marker TMRM (red). The horizontal bar represents 10 μm.

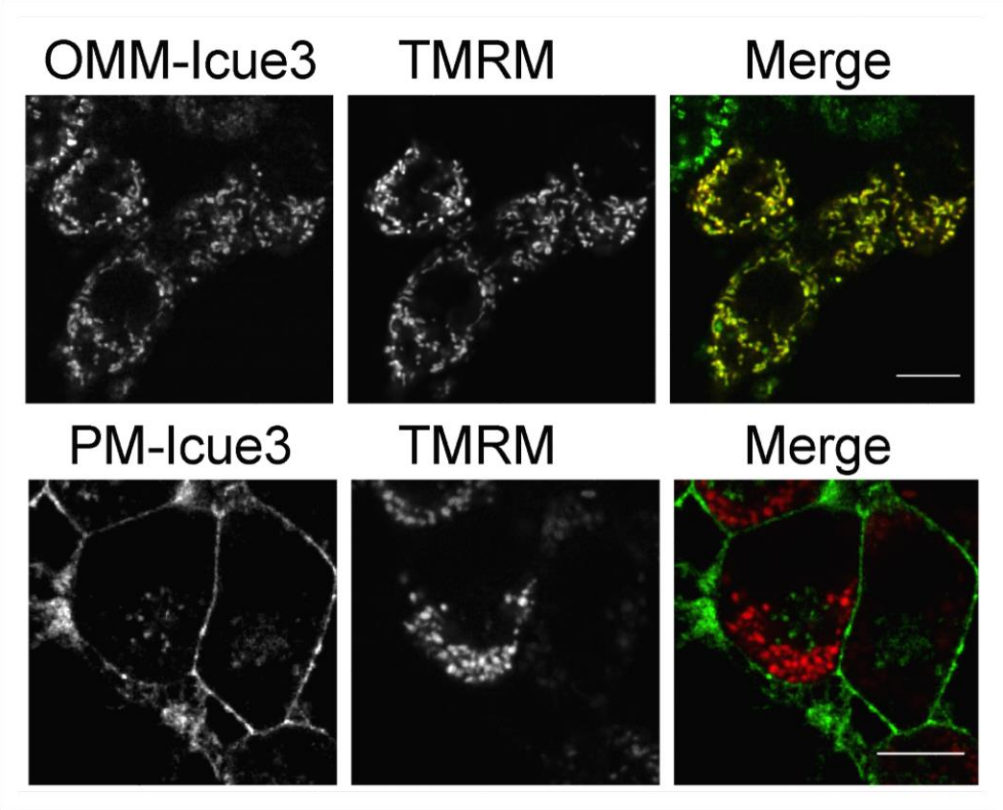

Supplementary Data Figure 6. cAMP sensor localizations. Confocal imaging of neuroblastoma N2a cells expressing the FRET-based cAMP sensors that localized either at the plasma membrane (PM-ICUE) or the outer mitochondrial membrane (Mito-ICUE). The horizontal bar represents 10 μm.

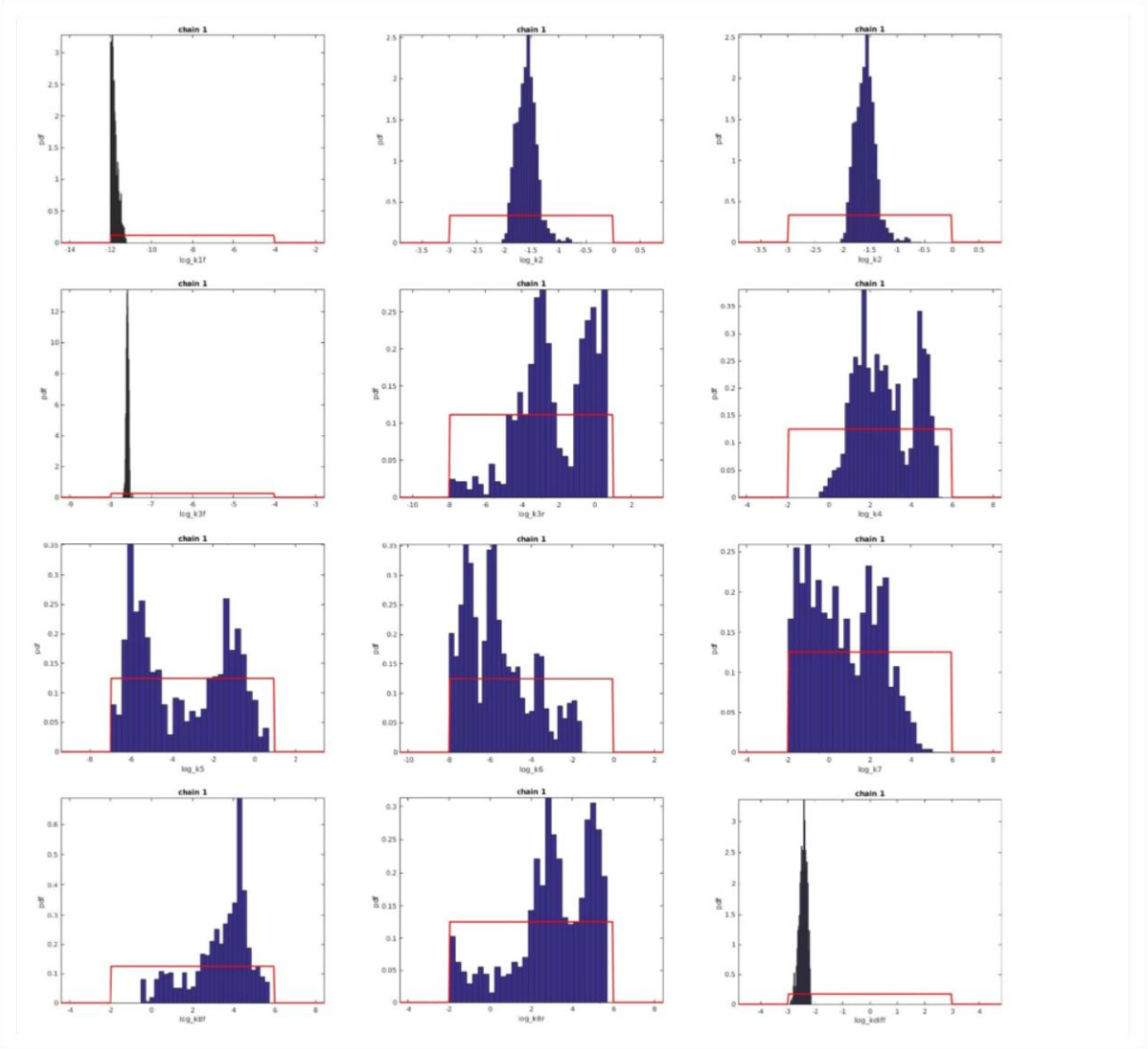

Supplementary Data Figure 7. Related to "Model constructions and analysis" section.

Histograms show parameter distributions for last 1000 swaps into the lowest chain of the replica exchange MCMC. Red outlines indicate naïve prior distributions.

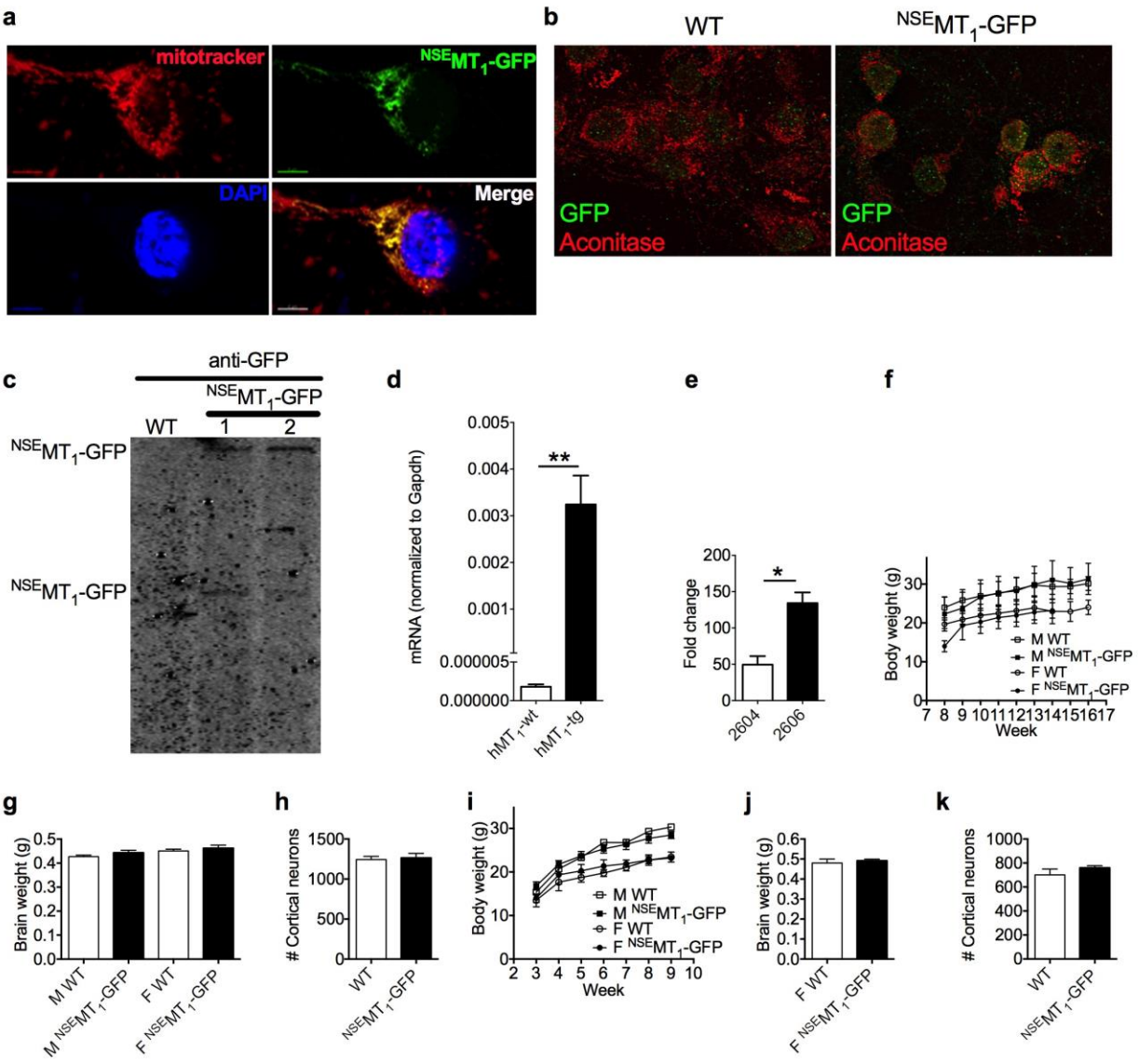

Supplementary Data Figure 8. Characterization of or NSE-MT$_1$ mouse. **a,** ^{NSE}MT1-GFP plasmid transfected primary cortical neurons were stained with mitotracker and counterstained with DAPI. Scale bar: 10µm. **b,** PCN from wild type (WT) and transgenic ^{NSE}MT1-GFP mice were stained using an anti-aconitase and anti-GFP antibodies. Background staining is appreciated in the nucleus of both, but specific GFP staining is detected in the transgenic mouse colocalizing with aconitase (mitochondrial marker). **c, d,** Expression of ^{NSE}MT$_1$-GFP transgenic protein (**c**) and real time PCR quantification of transgene from WT and ^{NSE}MT$_1$-GFP brains (**d**) was

determined. **e,** Fold change of transgene copy numbers in line 1 (2604) and 2 (2606) were measured using one primer which amplifies region that is conserved both in human and mouse. **f, i**, Body weights were measured between 8 and 17 weeks for line 1 (**f**), and between 3 and 17 weeks for line 2 (**i**). Brain weights and number of cortical neurons were compared using 8 weeks old mice for line 1 (**g, h**) and 2 (**j, k**) respectively.

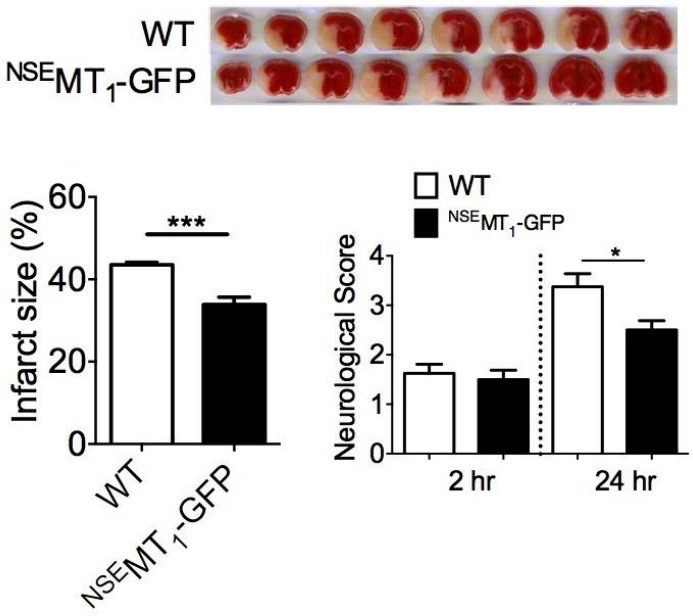

Supplementary Data Figure 9. Representative TTC staining of mice brains 24 hours after pMCAO in $^{NSE}MT_1$-GFP 2606 transgenic line. Infarct size has significant reduction in transgenic mice and neurologically, transgenic mice perform better than wild-type mice.

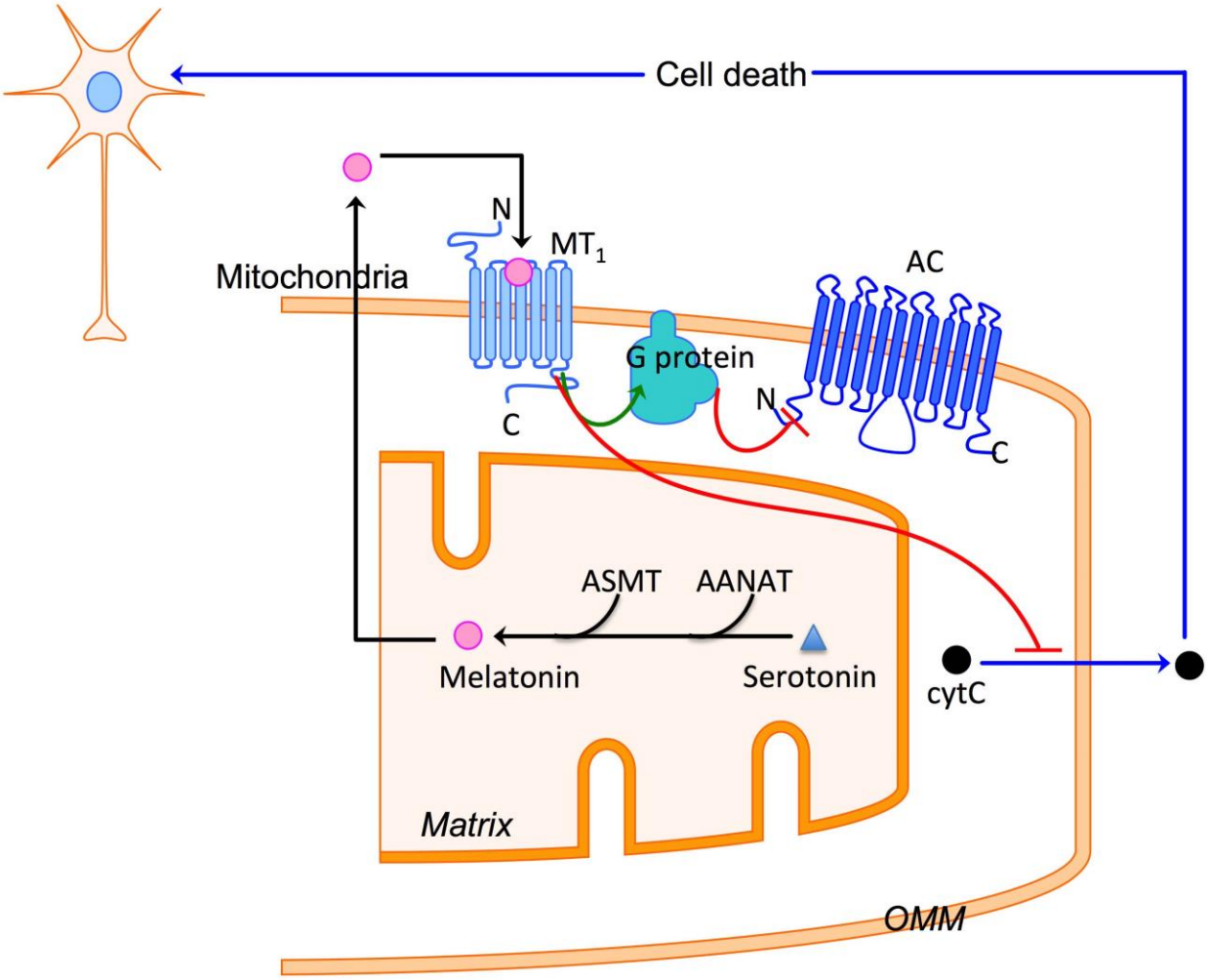

Supplementary Data Figure 10. Model of mitochondrial MT_1 signaling. Our data provide a mechanistic clue for understanding the neuroprotective action of melatonin. We propose that melatonin acts via an automitocrine pathway where the release of melatonin from the mitochondrial matrix acts directly in the mitochondrial MT_1/G-protein signaling system as a negative feedback mechanism that prevents cytochrome c release.

Supplementary Data Tables

Supplementary Data Table 1. Chemical reactions and rate constants for the model.

Reaction		Rate	Description
1	AC + ATP ⇆ AC.ATP	$k1_{forward}$,$k1_{rearward}$	cAMP production from AC
2	AC.ATP → AC + cAMP	k2	
3	PDE + cAMP ⇆ PDE.cAMP	$k3_f$,$k3_r$	cAMP degradation by PDE
4	PDE.cAMP →PDE + AMP	k4	
5	AMP →ATP	k5	
6	MTR + G_i → MTR.G_i	k6	Receptor/G protein coupling
	OR + G_i →OR.G_i		
7	MTR.G_i → MTR + G_i*	k7	G protein activation
	OR.Gi → OR + G_i*		
8	AC + Gi* ⇆ AC.G_i*	$k8_f$,$k8_r$	AC inhibition by active G protein

Supplementary Data Table 2. Initial quantities of molecular species in cytosol and mitochondria.

Species	Cyto/PM	Mito/OMM	References
MT_1	< 1.00E+06	1.13E+04 (MT_1)	
μOR	1.00E+06	0	
Gi	3.00E+06	3.39E+04	(1, 2)
AC	3.00E+05	3.39E+03	(1, 2)
PDE	2.40E+05	2.71E+03	(1)
ATP	1.00E+09	1.13E+07	(3)
cAMP	1.00E+07	1.13E+05	(4)

Supplementary Materials and Methods

Animals. The University of Pittsburgh Institutional Animal Care and Use Committee approved all experimental procedures, protocol #13112568. All procedures conformed to the National Institutes of Health Guide for the Care and Use of Laboratory Animals. In all experiments, we used male mice that were 8 to 10 weeks of age with 23 to 28 g body weight except otherwise indicated. Experimentally naïve wild-type (B6CBA), MT_1 male littermate mice maintained on a 12 h light/dark cycle were used as described (5). For the MT_1 mouse colony, MT_1 male mice were mated with F1 B6CBA females. All mice were adults unless otherwise specified.

Mitochondria isolation. Mouse brain tissue was homogenized and mitochondria were isolated according the published methods (5, 6). Briefly, tissue was homogenized using a Teflon

homogenizer and centrifuged at 1300 g for three minutes. Supernatant was collected and pellet resuspended and homogenized again. This was repeated two times. The resulting pellet (cellular debris and not homogenized tissue) was discarded and supernatants obtained from each individual homogenization/centrifugation step were pooled and used for further isolation of mitochondria. Both synaptosomal and non-synaptosomal mitochondria were isolated from wild-type and $^{NSE}MT_1$-GFP transgenic mice brain as described (5, 6). The purified mitochondria were then diluted into 1 mg/ml and treated with 10 μM melatonin or DMSO at 30ºC for 30 min, followed by pelleting the mitochondria at 6900 g. To ensure the purity of mitochondria, we verified plasma membrane, cytosol, endoplasmic reticulum contaminations with antibodies specific for these components of cells. For each experiment, five forebrains were pooled for mitochondria isolation. All experiments using isolated mouse brain mitochondria were done at least three times, for a total of 15 mice (n for each experiment in the figure legend, five pooled forebrains per n).

Immunoblot analysis. Briefly, 25 or 30 μg protein lysates were run on PAGE gels, transferred to PVDF-FL and probed with primary antibodies as follows: anti-Gαi (Abcam), anti-arrestin 1 and 2 (Santa Cruz Biotechnology), anti-$AANAT_{20-200}$ (3314, a generous gift from Dr. David C. Klein, NIH); anti-ASMT (bs-6961R, Bioss; 1:2000); anti-14-3-3ζ (AB 51129, Abcam; 1:2000), anti-TOM20 (Santa Cruz Biotechnology), anti-TIM23 (BD), anti-COXIV (Abcam), anti-β-actin (Sigma), anti-cytochrome c (Abcam), anti-Cadherin (Millipore), anti-Calreticulin (Millipore), anti-Syntaxin-6 (Cell Signaling), anti-Rab11 (Cell Signaling), anti-GFP (Sigma). Secondary antibodies were: Goat anti-rabbit (926-32211, LiCor, 1:20000); Goat anti-mouse (926-68020, LiCor, 1:20000). Blots were analyzed and quantified by fluorescence intensity on a LiCOR Odyssey.

Proteinase K digestion. Purified Mitochondria (25 or 100 µg) diluted in isolation buffer were incubated with proteinase K (10 µg/ml) for 0, 5, 15, 30 and 60 min in the presence or absence of digitonin (0.25%, w/v) at room temperature. The reaction was stopped by adding protease inhibitor cocktail (Roche). All samples were centrifuged at 12,000 g and 4 °C for 10 min. Each pellet was suspended in sample buffer and analyzed by immunoblot.

Pineal gland removal. Animals housed under a 12-h light, 12-h dark lighting regimen (lights on at 0700 h) were sacrificed at 1400 h for day pineal gland isolation (5-10 mice per experiment) and at 0200 h for night pineal gland isolation (5-10 mice per experiment). For night pineal gland removal, all procedures are carried out in the dark under a dim red safe light. The pineal glands are immediately homogenized in lysis buffer with protease inhibitors and frozen at -80 °C for later use. Brains are kept in mitochondrial isolation medium and mitochondria are isolated immediately after pineal gland removal. All homogenates are centrifuged and supernatants are used for immunoblot analysis.

Melatonin Synthesis. Isolated non-synaptosomal and synaptosomal mitochondria (1 mg/ml) were incubated with 50 µM d4-serotonin (58264-95-2, AlsaChim) or buffer alone (5 mM HEPES-Tris, 125 mM KCl, 2 mM Pi, 3 µM EDTA, 1 mM MgCl2, 1 mM ATP, 5 mM glutamate/malate, 5mM succinate, 10 µM deprenyl) for 30 minutes at room temperature, with total incubation volume of 100 µl. Sodium hydroxide (0.5 N, SS255, Fisher Chemical) was added to total volume of 1 ml. Melatonin and its intermediates were extracted using either chloroform (C2432, Sigma Aldrich) or acetonitrile. Then samples were dried down under nitrogen, and reconstituted in 100 µl ddH2O. Reconstituted samples are injected onto an Acquity UPLC BEH C18 column (2.1 X 100 mm) and eluted with 0.1% formic acid in water and acetonitrile using a gradient from 97:3 (initial) to 60:40 over five minutes and maintained 60:40

for one minute before re-equilibration at 97:3. Deuterated melatonin (d4) is detected in positive mode with a Thermo Fisher TSQ Quantum Ultra mass spectrometer interfaced via an electrospray ionization probe with the Waters UPLC Acquity solvent delivery system. Transitions used for analysis are 237 → 178 for d4 melatonin and 181 → 164 for d4 serotonin. Neat solutions (20 μM) of d4-serotonin, d4-melatonin (66521-38-8, AlsaChim), and n-acetyl-serotonin (1210-83-9, Sigma) were run to verify retention times and optimize detection.

AANAT knockout in N2a cells. Guide RNAs against mouse AANAT were designed and cloned into pLenti CRISPR vectors by the Magee Womens Research Institute Transgenic Core facility. The guide RNA sequences were TGATGTTCAACATGGGCGTC and GGGAGACAGCGGTTCCCAAC. N2a cells were co-transfected with pLenti AANAT-CRISPR A-eGFP and pLenti AANAT-CRISPR B-mCherry, using Lipofectamine2000 (Invitrogen) from Invitrogen according to the manufacturer's protocol. After 24 hr, cells were diluted and plated into 96-well plate as single cells. Single cells were cultured for around 10 days to obtain clonal cultures and then transfered to 6-well plate. AANAT knockout was verified using PCR (primer sequences: AANAT-F2 GAGAGAAAATCACGCTAACA; AANAT-R2 ATGCCACCATTAACAAGTC).

Primary cerebrocortical neuronal (PCNs) culture or N2a cells and oxygen/glucose deprivation (OGD). Culture of PCNs and OGD treatment of PCNs were performed as previously described (7). Briefly, the cerebral cortex of mouse embryos at day 15 (E15) were freed from meninges and separated from the olfactory bulb and hippocampus. Trypsinized cells were suspended in neurobasal medium (NBM) with 2% (vol/vol) B27 supplement, 2 mM glutamine, 100 units/ml penicillin and streptomycin (GIBCO, Carlsbad, CA) and seeded at a density of $2\times10^4/cm^2$ on poly-L-ysine-coated dishes. Cells were used for experiments on day 7 of

culture. PCNs or N2a cells were preincubated with or without melatonin at 10 μM or 40 μM concentration for 2 hours (PCNs) or 30 min (N2a cells), and subjected to OGD. For OGD, the culture medium was replaced by glucose-free Earle's balanced salt solution, and cells were placed in an anaerobic chamber, which was used to delete oxygen to <100 ppm within 90 min. Control cells were incubated in Earle's balanced salt solution with 25 mM glucose in a normoxic incubator for the same period. After 3 or 4 hours, OGD was terminated by a return to normal culture conditions. Cell death was determined by lactate dehydrogenase (LDH) assay.

Lactate dehydrogenase (LDH) assay. The extent of cell death was determined by the LDH assay according to the manufacturer's instructions (Roche Products). Briefly, each reaction mixture (100 μl) was added to conditioned media (100 μl) removed from dishes after centrifugation at 250 ×g for 10 min. Absorbance of samples at 490 nm was measured in a plate reader (Synergy H1) after 15 min of incubation at room temperature. The same volume of blank medium was used as the background control.

Cytochrome c release from N2a cells. Three 90% confluent 10 cm plates of N2a or N2a-AANAT KO cells were collected and washed with 1xPBS. The cell pellet was resuspended in 1 ml mitochondria isolation buffer (225 mM sucrose, 75 mM mannitol, 1 mM EGTA, 5 mM HEPES-Tris) and homogenized by passing through a 25G needle. The homogenates were then centrifuged at 800 g for 10 min. The supernatant was collected and centrifuged at 7000 g for 10 min. The resulting pellet was then collected and washed two times with mitochondria isolation buffer minus 1mM EGTA. The final crude mitochondria were diluted into 1 mg/ml and used for the cytochrome c release experiment. The concentration of cyclosporine A used was 10 μM.

Reactive Oxygen Quantification. N2a cells (WT and AANAT KO) plated in the same multiwell plates were incubated with 1 μM of MitoSOX reagent for 15 minutes. Cells were

washed with DMEM culture media and MitoSOX fluorescence was measured using λex/em=510/580 nm. The fluorescence intensity measured from cells without MitoSOX treatment were counted as background signal and was subtracted before analysis. Significance was assessed using paired sample t-test and found to be <0.001 (n=30).

MT_1-FLAG vectors construction and transfection: The vector mMT_1-FLAG was purchased from Origene (MR224599). The vector hMT_1-FLAG was created modifying the pcDNA3.1 DNA vector to hMT_1-FLAG-mCherry in our laboratory. The latter has the human MT1 CDS (hMT_1) in frame with the Flag tag and mCherry, under the CMV promoter of the pCDNA3.1 commercial plasmid. In order to remove the mCherry sequence, the vector hMT_1-FLAG-mCherry was digested with the restriction enzymes EcoRI and KpnI (New England Biolabs). The linearized plasmid was than ligated to annealed oligos carrying EcoRI and KpnI protruding ends and a stop codon in frame with the hMT_1 starting codon. The sequence of the product of the ligation reaction (T4 Ligase New England Biolabs) was confirmed by sequencing. The vector hMT_1-FLAG_$N_{4,10}$I was created by site-directed mutagenesis of the hMT_1-FLAG vector. We designed the primers MT_1Asn-Ile_mutag_For (aagcttatgcagggcaTcggcagcgcgctgcccaTcgcctcccagcccgtg) and MT_1Asn-Ile_mutag_Rev (cacgggctgggaggcgAtgggcagcgcgctgccgAtgccctgcataagctt), carrying two point mutations and we used hMT_1-FLAG vector as template for a PCR reaction. In order to digest the template, we treated the PCR product with the restriction enzyme DpnI (New England Biolabs) that digests only methylated DNA. The sequence of the PCR reaction product was confirmed by sequencing. The vectors were purified with the QIAGEN Plasmid Maxi Kit and the plasmidic DNA was used to transfect N2a plated on 150 mm dish. We used Lipofectamine 2000 (Invitrogen) as transfection reagent, following the manufacturer's protocol.

Confocal microscopy. Cells plated on coverslips were mounted in Attofluor cell chambers (Life Technologies) and incubated with Hepes buffer containing 150 mM NaCl, 10 mM Hepes, 2.5 mM KCl and 0.2 mM $CaCl_2$, 0.1% BSA, pH 7.4 were transferred on the Nikon Ti-E microscope (Nikon) equipped with a Z-driven piezo motor. Imaging were acquired using Nikon A1 confocal unit, through a 60X N.A=1.45 objective (Nikon) and using 440, 488, 514 and 560 nm lasers (Melles Griot), respectively. Emission fluorescence were acquired using a Spectral Detection mode and collected by a 32-channels PMT. Typically, a Z-stack of 4 to 8 images (Z step = 500 nm) was acquired every 5 minutes during 45 to 60 minutes. Data acquisitions were done using Nikon Element Software (Nikon Corporation). After acquisition, raw data were spectrally deconvoluted using Nikon Element Software (Nikon). Every different analysis was done at the single cell level.

Transmission Electron Microscopy (TEM). The specimens were fixed in cold 2.5% glutaraldehyde (25% glutaraldehyde EM grade, Taab Chemical) in 0.01 M PBS (sodium chloride, potassium chloride, sodium phosphate dibasic, potassium phosphate monobasic, Fisher), pH 7.3. The specimens were rinsed in PBS, post-fixed in 1% Osmium Tetroxide (Osmium Tetroxide crystals, Electron Microscopy Sciences) with 1% potassium ferricyanide (Potassium Ferricyanide, Fisher), dehydrated through a graded series of ethanol (30% - 90% - Reagent Alcohol, Fisher, and 100% - Ethanol 200 Proof, Pharmco) and embedded in Epon (Dodecenyl Succinic Anhydride, Nadic Methyl Anhydride, Scipoxy 812 Resin and Dimethylaminomethyl, Energy Beam Sciences). Semi-thin (300 nm) sections were cut on a Reichart Ultracut, stained with 0.5% Toluidine Blue (Toluidine Blue O and Sodium Borate, Fisher) and examined under the light microscope. Ultrathin sections (65 nm) were stained with 2% uranyl acetate (Uranyl Acetate dihydrate, Electron Microscopy Sciences, and methanol,

fisher) and Reynold's lead citrate (Lead Nitrate, Sodium Citrate and Sodium Hydroxide, Fisher) and examined on Jeol 1011 transmission electron microscope (grant # 1S10RR019003-01) with a side mount AMT 2k digital camera (Advanced Microscopy Techniques, Danvers, MA).

Immuno-Electron Microscopy (IEM). The specimens were fixed in cold 2.0% paraformaldehyde (paraformaldehyde Fisher), 0.01 % glutaraldehyde (25% glutaraldehyde EM grade, Taab Chemical) in 0.01 M PBS (sodium chloride, potassium chloride, sodium phosphate dibasic, potassium phosphate monobasic, Fisher), pH 7.3. The supernatant was removed and pelleted specimens were resuspended soluble10-15 µl of 3% gelatin in PBS (gelatin heated to 36°C prior to resuspension). Specimens were pelleted in this solution to concentrate them at the tip of the gelatin plug prior to gelling. Once solidified, the gelatin pellets were fixed further in the paraformaldehyde with glutaraldehyde fixative. The pellets were infused with 20% PVP 1.6 M Sucrose buffered with 0.055 M Sodium Carbonate overnight and then frozen to small stubs in liquid nitrogen. Semi-thin (300 nm) sections were cut on a Leica Ultracut 7 (grant # 1S10RR025488-01) with a cryokit at -90° C, stained with 0.5% Toluidine Blue (Toluidine Blue O and Sodium Borate, Fisher) and examined under the light microscope. Ultrathin sections (65 nm) were labeled with antibody and then visualized with a colloidal gold labeled secondary. After rinsing in PBS sections were fixed in 2.5% glutaraldehyde and then rinsed in PBS and dH2O. The rinsed sections were counterstained with 2% neutral uranyl acetate (Uranyl Acetate Dihydrate, Electron Microscopy Sciences) and 4% uranyl acetate, coated with methyl cellulose and examined on Jeol 1400 transmission electron microscope (grant #1S10RR016236-01) with a side mount AMT 2k digital camera (Advanced Microscopy Techniques, Danvers, MA).

Expansion Microscopy. Isolated mitochondria were placed on the coverslip, fixed with 4% PFA and permeabilized with 0.1% Triton X-100 for 5 min. Then mitochondria were incubated with a

combination of either anti-TOM20 and anti-FLAG or anti- TOM20 and anti -Aconitase antibodies t at 4C overnight. Then the mitochondria were incubated with secondary antibosies for 1h at RT and subjected to expansion procedure according to (8). Imaging was done using Olympus IX-81 fluorescent microscope equipped with UPLSAPO 100xO objective.

Immunofluorescence analysis of N2a, PCN, isolated mitochondria. Primary cortical neurons were fixed in 4% paraformaldehyde in PBS for 20 min, permeabilized with 0.1% Triton X-100 in PBS for 15 min at room temperature and subjected to immunofluorescence with the indicated primary antibodies. Secondary antibodies used are Alexa Fluor 488- or 594-conjugated anti-mouse or anti-rabbit IgG. Images were captured using a confocal laser scanning microscope system (FluoView FV1000; Olympus, Inc.). Isolated mitochondria were incubated with mitotracker deep red at 37 □C for 45 min. The mitotracker incubated mitochondria were then loaded onto the slide and fixed, followed by MT1 immunostaining. Images were taken using Olympus confocal laser scanning microscope (FluoView FV1000; Olympus, Inc.) equipped with 100x objective.

Assay for melatonin receptor binding affinity and expression in mitochondria. The affinity (Ki) of melatonin for melatonin receptors located in B6CBA wild-type mouse brain mitochondria (0.06-0.09 mg protein/tube) and plasma membrane (0.24-0.26 mg protein/tube) was assessed by competition binding analysis using 100 pM 2-[^{125}I]-iodomelatonin and 1 pM-100 nM melatonin as described (9). Total melatonin receptor expression (B_{max}) and affinity (K_d) of 2-[^{125I}]-iodomelatonin binding to melatonin receptors were assessed in mitochondria (0.06-0.22 mg protein/tube) and whole brain homogenates (0.25-0.46 mg protein per tube) by saturation isotherms using 0-500 pM 2-[^{125I}]-iodomelatonin for plasma membrane and 0-2.4 nM for mitochondria. Non-specific binding was determined using 10 μM melatonin. Parallel binding

assays were performed in the presence of 1 mM DTT using 250-500 pM 2-[I^{I25}]-iodomelatonin. Data were best fit analyzed by non-linear regression analysis least squares fit (Fig S4) (GraphPad Prism, Inc).

Time-course measurements of cAMP production in live neuroblastoma cells. Cyclic AMP was assessed using FRET-based assays. Cells were transiently transfected with FRET based biosensors for measuring cAMP either at the plasma membrane, the outer mitochondrial membrane (10), or the mitochondrial matrix (11). Measurements were performed and analyzed as previously described (12). In brief, cells plated on poly-D-lysine coated glass were mounted in Attofluor cell chambers (Life Technologies), maintained in Hepes buffer and transferred on the Nikon Ti-E equipped with an oil immersion 40X N.A 1.30 Plan Apo objective and a moving stage (Nikon Corporation). CFP and YFP were excited using a mercury lamp. Fluorescence emissions were filtered using a 480 ± 20 nm (CFP) and 535 ± 15 nm (YFP) filter set and collected simultaneously with a LUCAS EMCCD camera (Andor Technology) using a DualView 2 (Photometrics) with a beam splitter dichroic long pass of 505 nm. Fluorescence data were extract form single cell using Nikon Element Software (Nikon Corporation). The FRET ratio for single cells was calculated and corrected as previously described (13). Individual cells were continuously perfused with buffer or with the ligand for the time indicated by the horizontal bar.

Assay for cAMP measurement in isolated mitochondria. Cyclic AMP assay was performed on isolated mitochondria using the Direct cAMP ELISA kit (Enzo life science) according to the manufacturer's instructions in the absence or presence of melatonin or melatonin plus luzindole at 30ºC for 30 minutes.

***In vitro* cytochrome c release.** An aliquot of 100 µl of 1mg/ml mouse brain non-synaptosomal

mitochondria was pre-incubated with melatonin (10 µM) or melatonin plus luzindole (100 µM) for 5 min in mitochondria incubation buffer (125 mM KCl, 10 mM HEPES, 1 mM ATP, 5mM potassium succinate, 80 µM ADP, 2 mM K_2HPO_4), followed by incubation with 40 µM $CaCl_2$ at 30°C for 10 min. An aliquot of 25 µl were centrifuged at 10,000g at 4°C for 10 min. The supernatant and pellet (mitochondria) were evaluated by immunoblot. Alternatively, cytochrome c presence in the supernatant was also evaluated quantitatively using ELISA assay (Life Technologies).

Melatonin release from isolated mitochondria. Mitochondria pellet was resuspended in mitochondria incubation buffer (125 mM KCl, 10 mM HEPES, 1 mM ATP, 5mM potassium succinate, 80 µM ADP, 2 mM K_2HPO_4) to a final concentration of 1 mg/ml immediately after isolation. An aliquot of 500 µg was used as control or treated with 100 µM $CaCl_2$ at 30°C for 1 min followed by centrifugation at 7000 g for 2 min. Melatonin in the supernatant was extracted with chloroform and vacuum dried. The dried melatonin extracts were then resuspended in the diluted wash buffer and the quantification of melatonin was performed using melatonin ELISA kit according to the manufacturer's protocol (IBL International GMBH, Hamburg, Germany).

Caspase activity assay. Caspase-3 like activity was assayed by fluorometric protease assay kit according to manufacturer's instruction (Abcam). Briefly, tissue from ipsilateral brain of wild-type and $^{NSE}MT_1$-GFP mice at 24 hours after pMCAO were homogenized. Corresponding brain region of sham operated wild-type mice was used as control. The fluorescence intensity of cytosolic fraction was then quantified as caspase-3 activity by a plate reader (14).

Melatonin receptor 1 (MT_1) transgenic mouse. The Magee Womens Institute and Foundation Transgenic and Molecular Core facility generated two mouse lines overexpressing the human MT_1 selectively in neurons. We constructed and used a vector encoding the human MT_1 C-

terminally fused to the Flag-tag epitope and to eGFP, which is under the control of the neuronal specific enolase (NSE) promoter permitting a selective expression to the neurons. Vector construction was confirmed by sequencing. Transgenic mice were generated on the hybrid B6CBA background. Since B6CBA has normal endogenous melatonin levels, it will enable us to investigate signaling of both endogenous melatonin and exogenously added melatonin.

Permanent middle cerebral artery occlusion (MCAO). To minimize variation in endogenous melatonin levels, all experiments were performed at the same time each day between 9 am to 1 pm. For these experiments, we used permanent MCAO models in order to reflect the type of ischemic strokes seen in patients (15). Furthermore, we followed neurologic outcomes of mice up to 3 days in order to determine the effect of MT_1 on the survival of the neurons in the penumbra, which continue to be vulnerable after the first 24 hours of recovery from ischemia. Specifically, mice (body weight 23-28 g) was given 2% isofluorane in 28% oxygen and 70% nitrous oxide using a face mask, and anesthesia was maintained with 0.5-1% isofluorane throughout the procedure. Rectal temperature of mice was maintained at 37 ± 0.5˚C with a feedback-controlled heating blanket (Harvard Apparatus) during the surgery. Mice were placed in the supine position. Following a midline skin incision, the left common carotid artery, the external carotid artery, and the internal carotid artery were exposed, dissected free from surrounding tissue, and their branches were electrocoagulated. The external carotid artery was dissected further distally and coagulated. Focal cerebral ischemia was induced by an intraluminal 6-0 nylon monofilament thread coated with a silicone tip (180 μm diameter) introduced through a small incision on the left external carotid artery into the left internal carotid artery. The silicone-coated suture was inserted 9 ± 1 mm into the internal carotid artery up to the origin of the middle cerebral artery. The suture was then fixed by ligation to the stump of the external

carotid artery proximal to the common carotid bifurcation. The wound was then closed. The suture was left in place in order to permanently occlude the middle cerebral artery until the mice are sacrificed. A laser Doppler probe adhered to the left temporal aspect of the skull (5 mm lateral and 2 mm posterior to bregma) was used to monitor arterial flow disruption. To prevent hypothermia after surgery, the mice were kept warm in a temperature-controlled unit until the mice were completely awake. Control mice undergo sham surgery consisting only of anesthesia and carotid artery dissection. Animals were allowed to recover, and neurologically evaluated at 2, 24, and 72 hours following MCAO.

Infarction volume and neurological deficits. After slicing with mouse brain matrix, the brain slices (1mm thick) were then stained with 2% 2,3,5-triphenyltetrazolium chloride (TTC) for 10 min in a 37 °C water bath (16). Areas that were not stained red with TTC were identified as the infarct area. After staining, the brain slices were fixed with 4% paraformaldehyde for 30 min and scanned. The TTC stained areas of the ipsi- and contralateral hemispheres were quantified separately with ImageJ. The infarct area was indirectly calculated by subtracting the area of intact tissue in the ipsilateral hemisphere from that in the contralateral hemisphere. These values were then used to calculate the infarct volume expressed as a percentage of the contralateral hemisphere. Each animal was assessed for neurological deficits at 2 and 24 hours or 72 hours after onset of focal ischemia. The following scoring was used: 0, no observable deficits; 1, forelimb flexion when lifted by the tail; 2, forelimb flexion and consistently reduced resistance to lateral push; 3, forelimb flexion, reduced resistance to lateral push, and unilateral circling toward the paretic side; 4, forelimb flexion and ambulation inability or difficulty; 5, dead (15, 17).

Analysis of Cytochrome c release from tissue samples. Wild type and transgenic mouse brains were removed and ipsilateral hemisphere was dissected at 24 hours after occlusion.

Corresponding region of wild type brain from sham operated mouse was separated as well. Dissected tissues were immediately kept in mitochondria isolation buffer (300 ul buffer per 100 mg tissue) on ice as stated above in mitochondria isolation section. Tissues were then homogenized and centrifuged at 1300 g. Supernatants were collected and centrifuged again at 7000 g for 10 min. The resulting supernatants were used for the quantification of released cytochrome c. The amount of cytochrome c release was measured by cytochrome c ELISA assay (Life Technologies).

qPCR. WT or MT_1 mouse brain was isolated at eight weeks of age and lysed for total RNA using an RNAEasy (Qiagen) kit. Reverse transcription PCR (RT-PCR) was done using a high capacity RNA to cDNA kit (Applied Biosystems). The cDNA products of RT-PCR were then amplified (BioRad CFX97 Touch) using RT^2 qPCR primer assay from QIAGEN (Cat. #: PPH02532A; PPM02946E) and mRNA expression was quantified using the ΔΔCt method (18). In addition, to amplify both mouse and human MT_1, we used the following primer: forward, 5'-ACCATCGTGGTGGACAT-3', reverse, 5'-GTTCCTGAGCTTCTTGTT-3'.

Model constructions and analysis. We constructed a simple mathematical model of the proposed mechanism (Supplementary Data Fig. 7). Forskolin treated cells have active adenylyl cyclases (AC) on both the plasma membrane (PM) and the outer mitochondrial membrane (OMM). Active AC localized to the PM converts cytosolic ATP to cytosolic cAMP; active AC on the OMM converts ATP in the mitochondrial lumen (ML) to luminal cAMP. Nucleotides were permitted to diffuse through the OMM, but proteins were constrained to their cellular compartments. Cyclic AMP in the cytosol and ML was converted via phosphodiesterases (PDE) to AMP, which was converted to ATP. In forskolin treated cells under steady-state conditions, relative ATP and cAMP levels were therefore regulated by AC and PDE activity.

MT_1 and μOR were overexpressed and localized to the plasma membrane. MT_1 also localizes to the OMM, but μOR did not. Upon stimulation with a saturating concentration of DAMGO, μOR became active and activates cytosolic Gαi proteins. Active Gαi bound to membrane AC, where it inhibited the conversion of ATP to cAMP. Similarly, stimulation with saturating quantities of melatonin initiated activation of MT_1 at both the plasma membrane and the outer mitochondrial membrane. MT_1-activated Gαi inhibited cAMP production in both the cytosol and the ML.

The model was constructed in compartmental BioNetGen (19) and assumes mass action kinetics. The cell was modeled as a sphere with 1pL volume, containing 100 mitochondria, each represented as a sphere with 0.3 μm radius. For simplicity, it was assumed that protein concentrations in the ML were identical to those in the cytosol. Similarly, the AC density on the OMM was the same as on the PM; however, the concentrations of MT_1 on the OMM and on the PM were independent. It was further assumed that the kinetics of Gαi activation by μOR and MT_1 were identical. The final model contains 30 molecular species, the time evolution of which was governed by 30 ODEs containing 12 kinetic parameters (Supplementary Data Table 1). Initial quantities of Gαi, AC, PDE, ATP and cAMP were assigned in the cytosol or PM as shown in Supplementary Data Table 2. Mitochondrial quantities were scaled by volume. As equilibrium quantities of all molecular species depend on the rate constants, the model was executed in the absence of MT_1 and μOR until steady state was reached. To simulate the effect of a saturating concentration of DAMGO, the model was initialized using equilibrium concentrations of all molecular species, plus 10^6 active copies of μOR on the PM (approximately $2068/\mu m^2$). No active MT_1 was present in the case of DAMGO stimulation. To simulate melatonin stimulation, equilibrium concentrations of all molecular species were used, plus 2068 MT_1 per square μm of OMM. MT_1 concentrations on the PM were less than or equal to this, and the concentration ratio

$[MT_{1PM}]/[MT_{1OMM}]$ was a free parameter of the model.

Model parameters were simultaneously fit to data from both experiments using a parallel tempering algorithm in which eight replicate Markov chains were run in parallel at various temperatures, and 10,000 exchanges between chains were performed. For each trial parameter set, the model was equilibrated and both experiments were simulated. Performance was assessed by fitting the model trajectory to the time evolution of cytosolic and mitochondrial cAMP.

Statistical analysis. Quantitative data were expressed as the mean value ± s.d. or s.e.m. as indicated. Statistical comparisons were conducted using ANOVA for multiple comparisons or student's t-test for difference between two conditions. Differences with $P < 0.05$ were considered statistically significant.

References for Supplementary Methods

1. Neves SR, *et al.* (2008) Cell shape and negative links in regulatory motifs together control spatial information flow in signaling networks. *Cell* 133(4):666-680.
2. Post SR, Hilal-Dandan R, Urasawa K, Brunton LL, & Insel PA (1995) Quantification of signalling components and amplification in the beta-adrenergic-receptor-adenylate cyclase pathway in isolated adult rat ventricular myocytes. *The Biochemical journal* 311 (Pt 1):75-80.
3. Huang H, *et al.* (2010) Physiological levels of ATP negatively regulate proteasome function. *Cell Res* 20(12):1372-1385.
4. Sudlow LC & Gillette R (1997) Cyclic AMP levels, adenylyl cyclase activity, and their stimulation by serotonin quantified in intact neurons. *The Journal of general physiology* 110(3):243-255.

5. Yano H, *et al.* (2014) Inhibition of mitochondrial protein import by mutant huntingtin. *Nat Neurosci* 17(6):822-831.

6. Kristian T (2010) Isolation of mitochondria from the CNS. *Current protocols in neuroscience / editorial board, Jacqueline N. Crawley ... [et al.]* Chapter 7:Unit 7 22.

7. Wang X, *et al.* (2011) The melatonin MT1 receptor axis modulates mutant Huntingtin-mediated toxicity. *J Neurosci* 31(41):14496-14507.

8. Tillberg PW, *et al.* (2016) Protein-retention expansion microscopy of cells and tissues labeled using standard fluorescent proteins and antibodies. *Nat Biotechnol* 34(9):987-992.

9. Witt-Enderby PA & Dubocovich ML (1996) Characterization and regulation of the human ML1A melatonin receptor stably expressed in Chinese hamster ovary cells. *Mol Pharmacol* 50(1):166-174.

10. DiPilato LM, Cheng X, & Zhang J (2004) Fluorescent indicators of cAMP and Epac activation reveal differential dynamics of cAMP signaling within discrete subcellular compartments. *Proc Natl Acad Sci U S A* 101(47):16513-16518.

11. Di Benedetto G, Scalzotto E, Mongillo M, & Pozzan T (2013) Mitochondrial Ca(2)(+) uptake induces cyclic AMP generation in the matrix and modulates organelle ATP levels. *Cell metabolism* 17(6):965-975.

12. Ferrandon S, *et al.* (2009) Sustained cyclic AMP production by parathyroid hormone receptor endocytosis. *Nat Chem Biol* 5(10):734-742.

13. Vilardaga JP (2011) Studying ligand efficacy at G protein-coupled receptors using FRET. *Methods Mol Biol* 756:133-148.

14. Zhang Y, *et al.* (2006) Huntingtin inhibits caspase-3 activation. *EMBO J* 25(24):5896-5906.

15. Friedlander RM, *et al.* (1997) Expression of a dominant negative mutant of interleukin-1 beta converting enzyme in transgenic mice prevents neuronal cell death induced by trophic factor withdrawal and ischemic brain injury. *J Exp Med* 185(5):933-940.

16. Suofu Y, *et al.* (2012) Matrix metalloproteinase-2 or -9 deletions protect against hemorrhagic transformation during early stage of cerebral ischemia and reperfusion. *Neuroscience* 212:180-189.

17. Hara H, *et al.* (1997) Inhibition of interleukin 1beta converting enzyme family proteases reduces ischemic and excitotoxic neuronal damage. *Proc Natl Acad Sci U S A* 94(5):2007-2012.

18. Yeatts K (2011) Quantitative polymerase chain reaction using the comparative C q method. *Methods Mol Biol* 700:171-184.

19. Faeder JR, Blinov ML, & Hlavacek WS (2009) Rule-based modeling of biochemical systems with BioNetGen. *Methods Mol Biol* 500:113-167.